ELECTRONIC SUPPLEMENTARY INFORMATION

A spectIR-fluidic reactor for monitoring fast chemical reaction kinetics with on-chip attenuated total reflection Fourier transform infrared spectroscopy

Nan Jia,[a] Leon Torres de Oliveira,[a] André Bégin-Drolet[b] and Jesse Greener [a,c]*

[a] Département de chimie, Faculté des sciences et de génie, Université Laval, Québec, QC G1V 0A6, Canada

[b] Département de génie mécanique, Faculté des sciences et de génie, Université Laval, Québec, QC G1V 0A6, Canada

[c] CHU de Québec, centre de recherche du CHU de Québec, Université Laval, Québec, QC G1L 3L5, Canada

Corresponding author: Jesse.Greener@chm.ulaval.ca

Section S1—Flow simulations:

Computational fluid dynamics simulations (COMSOL Multiphysics V5.4, Stockholm, Sweden) were used to determine the flow velocities and concentration profile under steady state. This was achieved by using the laminar flow and transport of diluted species modules. For momentum transfer parameters, boundary conditions of Navier-slip were used on channel walls, applying a no-penetration rule to the wall with $v \cdot n_{wall} = 0$, as well as adding a friction force (F_{fr}) to them in the form $F_{fr} = -\frac{\mu}{\beta} v$, where μ s the dynamic viscosity, v is the flow velocity vector, and β is the slip length. A slip length of 70% of the minimum mesh element length was used. Zero-gauge pressure condition was set at the outlet, and 0.00247 m s^{-1} velocity profile (equivalent to a flow rate of 0.3 mL hr^{-1}) at the inlet. Initial condition of zero velocity and zero-gauge pressure were set.

For mass transfer parameters, the boundary condition of 0.2 M and 0.0631 M were set for the phosphate and hydrochloric acid inlets, respectively. Flux (Danckwerts) constraints were applied at the inlets to improve stability. An outflow condition was applied at the outlet, assuming convection transport is predominant and ignoring diffusive transport at the border. Diffusion coefficients of D_{HPO4-} = 0.69×10^{-9} m^2 s^{-1} and D_{H+} = 9.31×10^{-9} m^2 s^{-1} were used for phosphate and hydrogen ions respectively. An initial condition of neutral pH (pH = 7) was set for the simulation. A steady-state simulation was run of an incompressible Newtonian fluid under isothermal laminar flow conditions. After discretizing the geometry and applying the required boundary conditions, the governing equations were solved. As a result, the mass conservation (continuity, Eqn. S1), momentum conservation (Navier–Stokes, Eqns. S2 and S3), and mass transport (Fick's law, Eqns. S4 and S5) equations used to model 2D flow in the channels are simplified into the following equations:

$$\rho\nabla(\vec{v}) = 0 \qquad \text{Eqn. S1}$$

$$\rho(\vec{v}\cdot\nabla)\vec{v} = \nabla\cdot[-p\cdot\mathbf{I}+\mathbf{K}] + F \qquad \text{Eqn. S2}$$

$$\mathbf{K} = \mu(\nabla\vec{v} + (\nabla\vec{v})^{T}) \qquad \text{Eqn. S3}$$

$$\nabla\cdot J_i + \vec{v}\cdot\nabla c_i = 0 \qquad \text{Eqn. S4}$$

$$J_i = -D_i\nabla c_i \qquad \text{Eqn. S5}$$

where ∇ is the spatial gradient operator, $\vec{v}$ is the three-dimensional velocity field (m s^{-1}), ρ is the fluid density (kg m^{-3}), p is the pressure (Pa), μ is the dynamic viscosity (Pa s), F is the volumetric force vector (N m^{-3}), $\mathbf{K}$ is the viscous stress tensor (Pa), $\mathbf{I}$ is an identity matrix, J_i is the diffusive flux vector (mol m^{-2} s^{-1}), D_i is the diffusion coefficient (m^2 s^{-1}), and c_i is the concentration (mol m^{-3}). The subscript i refers to each component used in the simulation (phosphate and hydrogen ions).

A triangular mesh was built with a total of 399452 elements, covering the entirety of the geometry. The PARDISO numerical solver was used to solve the system, and the relative tolerance for the convergence criteria value was 0.001.

Section S2—Reynolds number:

The Reynold's number in an rectangular channel can be calculated by the equation:

$$R_e = \frac{\rho v d_H}{\mu} \quad \text{(Eqn. S6)}$$

where ρ is liquid density, v is velocity, μ is kinematic viscosity and d_H is hydraulic diameter. For rectangular channel, hydraulic diameter can be calculated using follow equation:

$$d_H = \frac{4 \times A}{P} = \frac{4 \times a \times b}{2 \times (a+b)} \quad \text{(Eqn. S7)}$$

whereas A is cross section area, P is wetted perimeter, a and b are width and height of the cross section, respectively.

Given Q_T =16 mL h^{-1}, we can get Reynold's numbers in mixing channel and in reaction switchback channels are 11.8 and 16.1, respectively. Similarly, for Q_T =1.3 mL h^{-1}, the Reynold's numbers in mixing channel and in reaction switchback channels are 4.8 and 6.6, respectively.

In summary, flow is highly laminar in all locations within the device at all both flow rates used in this work.

Section S3—Stray light problem in unmixed co-flowing streams

Here we discuss a measurement error that can occur in the case that an improperly mixed reaction stream is monitored spectroscopically. In the most extreme case, completely un-mixed reagents streams will co-flow side-by-side, with one of those streams being highly absorbing and the other being unabsorbing. Since in this work, each arm of the reaction channel is measured across nearly the entire channel cross-section the absorbance measurement will include both reagent streams (Figure S1a). As shown below, the absorbance ($A=-\log(I/I_0)$) from this situation can differ from the average absorption value if the absorbance of the low concentration side (A_B, Figure S1b) were averaged with the absorbance of the high concentration side (A_A, Figure S1c). We assume that the inbound light has the same intensity on both sides $I_{A0}=I_{B0}$, which is a fair assumption based on the narrow aperture admitting nearly uniform light across its short access. The light intensity after crossing channel will be I_A and I_B. As $stream_A$ contains the molecules that we monitored (HPO_4^{2-}), we assume that it will absorb light, while stream B does not ($I_{B0}=I_B$).

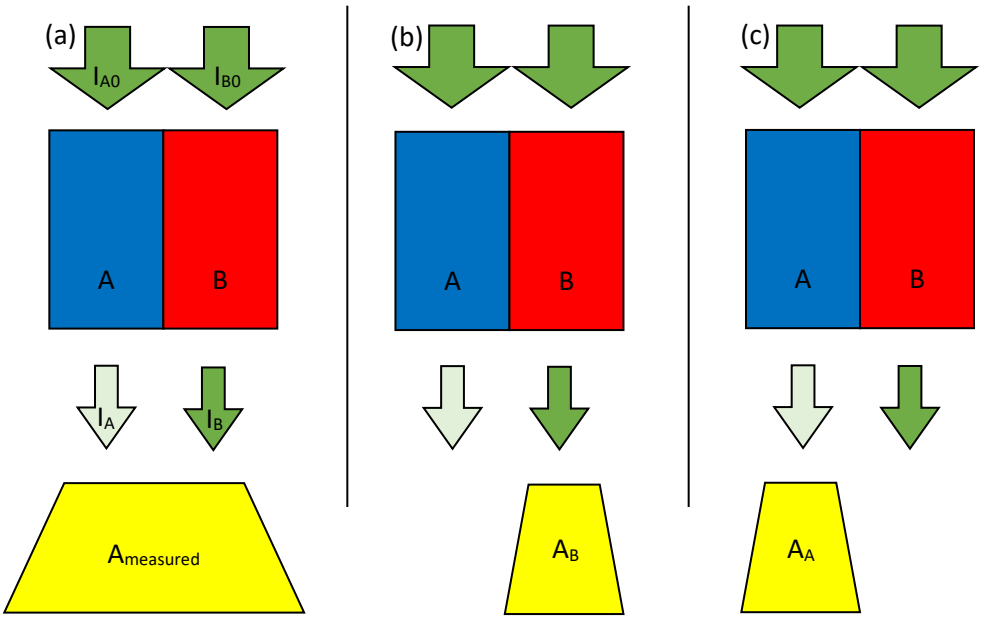

Figure S1. A schematic showing the stray light principle, in which light shining through a region of high and low absorbance can lead to errors in the average absorbance if they are detected simultaneously (a) when compared to the average absorbance obtained individually from the low absorbing side (b), and the highly absorbing side (c).

Monitoring I_A and I_B separately, as the schematic image above, would give absorbance A_A and A_B separately, and the real absorbance of the two sides would be A_{real}, given by the average absorbance:

$$A_{real} = \frac{1}{2}(A_A + A_B) = -\frac{1}{2}\left(\log\frac{I_A}{I_{A0}} + \log\frac{I_B}{I_{B0}}\right) = -\frac{1}{2}\left(\log\frac{I_A}{I_{A0}} + 0\right) = -\frac{1}{2}\left(\log\frac{I_A}{I_{A0}}\right) \quad \text{(Eqn. S8)}$$

In our system, the measured absorbance will be $A_{measured}$, which is given by the following equation:

$$A_{measured} = -\log\left(\frac{I_A + I_B}{I_{A0} + I_{B0}}\right) \quad \text{(Eqn. S9)}$$

As we assumed before, $I_{A0} = I_{B0} = I_B$,

$$A_{measured} = -\log\left(\frac{I_A + I_{A0}}{I_{A0} + I_{A0}}\right) = -\log\left(\frac{I_A}{2I_{A0}} + \frac{I_{A0}}{2I_{A0}}\right) = -\log\left(\frac{I_A}{2I_{A0}} + \frac{1}{2}\right) \quad \text{(Eqn. S10)}$$

With the two equations about A_{real} and $A_{measured}$, we can obtain A_{real} and $A_{measured}$ at certain value of I_A. We set $I_{A0} = 1$ and vary I_A between 0.99 and 0.60, to obtain the calculated values of A_{real} and $A_{measured}$ which are plotted in Figure S2:

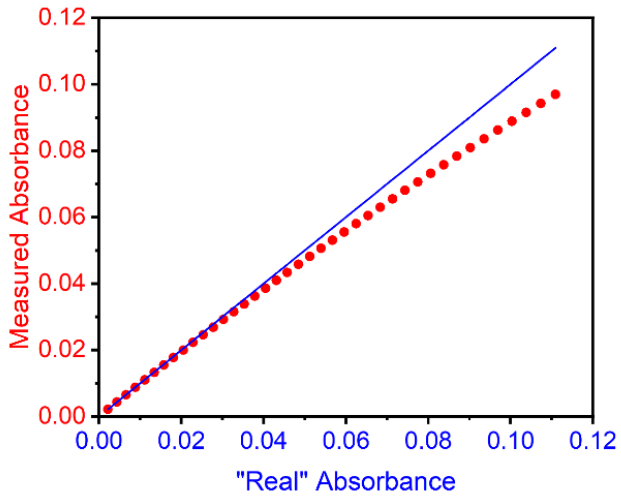

Figure S2. A plot of measured absorbance ($A_{measured}$) versus the real absorbance (A_{real}) using equations S9 and S10. A blue line shows the ideal linear relationship between $A_{measured}$ and A_{real}.

If we plot $A_{measured}$ vs. Areal (red dot) we can see that at high absorbance it deviates from a straight line (blue line) which should have an ideal slope of 1 everywhere. This is the nature of the stray light error. However, for low absorbing solutions A_{real} and $A_{measured}$ converge to the same linear curve at measured absorbances of less than 0.03. As this work deals with weakly absorbing solutions, with $A_{measured}$<0.03 it is assumed that this study does not suffer from the stray light problem. It is also work reminding that the this is an extreme example in which solutions are completely unmixed. Therefore, for real examples with partially mixed solutions, the two curves in Figure S2 will converge at higher absorbance values. We recommend for future studies using the appropriate (smaller) apertures for the SpectIR-fluidic reactor to obtain A_A and A_B measurements independently on each side of the channel at the most upstream location (where mixing is the least developed) to determine the threshold for onset of the stray light error.